Journal of Nuclear Materials 392 (2009) 176–183

Contents lists available at ScienceDirect

Journal of Nuclear Materials

journal homepage: www.elsevier.com/locate/jnucmat

The EBR-II X501 minor actinide burning experiment

M.K. Meyer [a], S.L. Hayes [a], W.J. Carmack [a,*], H. Tsai [b]

[a] Nuclear Fuels and Materials Division, Idaho National Laboratory, P.O. Box 1625, Idaho Falls, ID 83415-6188, USA
[b] Argonne National Laboratory, 9700 S. Cass Avenue, Argonne, Il 60439-4803, USA

A B S T R A C T

The X501 experiment was conducted in EBR-II as part of the integral fast reactor (IFR) program to demonstrate minor actinide (MA) burning through the use of a homogeneous recycle scheme. Renewed interest in the behavior of MA's during fuel irradiation has prompted further examination of existing X501 data, and generation of new data where needed in support of the US waste transmutation effort. The X501 experiment is one of the few MA-bearing fuel irradiation tests conducted worldwide and knowledge can be gained by understanding the changes in fuel behavior due to addition of MA's. Of primary interest are the affect of the MA's on fuel-cladding-chemical-interaction, and the redistribution behavior of americium. The quantity of helium gas release from the fuel and any effects of helium on fuel performance are also of interest. This paper provides a summary of the X501 fabrication, characterization, irradiation, and postirradiation examination.

1. Introduction

The X501 experiment was conducted in EBR-II as part of the integral fast reactor (IFR) program to demonstrate minor actinide (MA) burning through the use of a homogeneous recycle scheme. The X501 subassembly contained two metallic fuel elements loaded with relatively small quantities of americium and neptunium. Interest in the behavior of minor actinides (MA) during fuel irradiation has prompted further examination of existing X501 data, and generation of new data where needed in support of the US waste transmutation effort. The X501 experiment is one of the few minor actinide-bearing fuel irradiation tests conducted worldwide and knowledge can be gained by understanding the changes in fuel behavior due to addition of MA's. Of primary interest are the affect of the MA's on fuel-cladding-chemical-interaction, and the redistribution behavior of americium. The quantity of helium gas release from the fuel and any effects of helium on fuel performance are also of interest. It must be stressed that information presented at this time is based on the limited PIE conducted in 1995–1996, and currently represents a set of observations rather than a complete understanding of fuel behavior.

The original concept of the IFR incorporated a passively safe reactor design with on-site fuel recycling [1]. The IFR process utilized pyroprocessing of metallic fuel to separate U, Pu, and the MA (Am, Np, and Cm) from the non-actinide constituents. The actinides are reintroduced into the fuel and re-irradiated. Spent IFR fuel was expected to contain low levels of the MA because the hard neutron spectrum should transmute these isotopes as they are produced. This opens the possibility of using an IFR to transmute actinide waste from spent light water reactor (LWR) fuel. Elimination of actinides from spent LWR fuel, which is destined for the high level waste (HLW) repository, would reduce the radiotoxicity of material requiring long-term storage and isolation [2,3]. Reducing the levels of actinides in HLW would make the performance criteria of the repository easier to attain. A standard IFR fuel was based on the alloy U–20%Pu–10%Zr (wt%). The metallic fuel system eases the requirements for reprocessing methods and enables the MA metals to be incorporated into the fuel with simple modifications to the basic fuel casting process. The nominal fuel composition used in the X501 experiment was U–20.3%Pu–10.0%Zr–2.1%Am–1.3%Np and is based on a concept where the standard IFR fuel is fabricated with Pu extracted from spent LWR fuel which has cooled 10 years. The LWR fuel is then envisioned to have gone through a reprocessing scheme during which the MA accompanies the Pu through the processing steps. About 0.12 wt% of Cm would also be present, but the radiation protection difficulties created by handling Cm outside of a hot cell and the low alloying content eliminated Cm from inclusion in these experiments. In this paper we report the initial casting experience of IFR fuel containing MA, the irradiation conditions for the X501 experiment, and a summary of the postirradiation examination of the two MA-bearing pins of the X501 experiment.

1.1. X501 fabrication

Metallic U–20%Pu–10%Zr (by weight) nuclear fuel was differential pressure injection cast into a vitreous silica mold with the addition of two MA's, 2.1%Am and 1.3%Np. Three full length fuel

* Corresponding author. Tel.: +1 208 526 6360; fax: +1 208 526 0990.
E-mail address: Jon.Carmack@inl.gov (W.J. Carmack).

0022-3115/$ - see front matter © 2009 Elsevier B.V. All rights reserved.
doi:10.1016/j.jnucmat.2009.03.041

slugs (4.3 × 340 mm) were successfully cast incorporating both Np and Am. No unusual macrosegregation of the major constituents was observed. About 60% of the initial Am and 100% of the Np charge was present in the as-cast fuel. Am loss was attributed to volatile contaminants in the feed stock and evaporation at the casting temperature (1465 °C). Minimal loss of Am is experienced when volatile contaminants are not present and the Am is properly incorporated into the melt. Microstructural and microchemical characterization of the as-cast fuel along with bulk chemical analyses are reported. Details of the casting process and resulting microstructure are given in reference [4]. Considerable americium was lost due to volatilization during the fabrication process, which was not designed for use with Am-bearing alloys.

2. Materials and methods

The typical injection casting temperature for U–20%Pu–10%Zr is 1465 °C. The superheat is about 150 °C which is required to fill the molds which are 4.3 × 460 mm. The feed stock used was elemental metallic Np, U, Zr, and Pu. The Am feed stock was a metallic alloy of Pu–20%Am. Potential concerns in casting metallic fuels with minor actinide elements were the wide variations in vapor pressure between Am, Np, Pu and U, and the very highly negative free energy of oxide formation for Am. Over the range of melting temperatures, Am has nearly three orders of magnitude higher vapor pressure than Pu, and five orders of magnitude higher than Np or U [5,6]. This implies that a significant amount of Am could be lost as a vapor at casting temperatures. The potential for Am oxidation arises because AmO is considerably more stable than ZrO, UO, or PuO, at all temperatures [7]. It is possible that the Am could become part of the casting dross and not be incorporated into the fuel. The challenge becomes how to cast these fuel alloys with minimum Am loss under the characteristic range of processing conditions.

In order to reduce Am loss through evaporation and reaction with oxygen, the time at elevated temperatures, where the Am evaporation and reaction rates are high, should be constrained to as short as possible. The fabrication facility (the Experimental Fuels Laboratory at Argonne National Laboratory in Idaho) was therefore modified to include a bucket device with a lid allowing the Pu–Am feed material to be added to molten fuel within the crucible late in the melt cycle to minimize the time at temperature. Furthermore, the atmosphere above the melt was extremely pure Ar (99.9997%), containing less than 1.5 ppm oxygen. The elements (U, Zr, Np and some Pu) were loaded into a Y_2O_3 coated graphite crucible and induction heated under an Ar atmosphere. After reaching a temperature of 1495 °C, the melt was stirred causing the temperature to drop to 1465 °C. The melt was reheated and stirred again. At this point, the Pu–Am was added to the crucible via the bucket which sat next to and above the crucible inside the furnace. When the Pu–Am feed stock was added, 'sparks' were observed emerging from the melt. Casting proceeded and three full length pins were successfully cast into zirconium oxide coated quartz molds. The entire crucible charge was consumed during casting and the pins were removed from the molds. Two pins were encapsulated and made ready for in-reactor (EBR-II) testing while the remaining pin was sacrificed for metallographic and chemical characterization.

3. Fabrication results

Fig. 1 shows optical images of fuel cross-sections taken from locations near the top and bottom of a pin from the same casting batch as the irradiated fuel pins. Fig. 1(a) was taken from the top section of the fuel pin, and shows the inhomogeneous structure typical of U–Pu–Zr fuel produced by this casting method. Fig. 1(b) shows a micrograph of a section taken from the lower part of the fuel pin, in a region where cooling is slower after solidification due to proximity to the furnace internals.

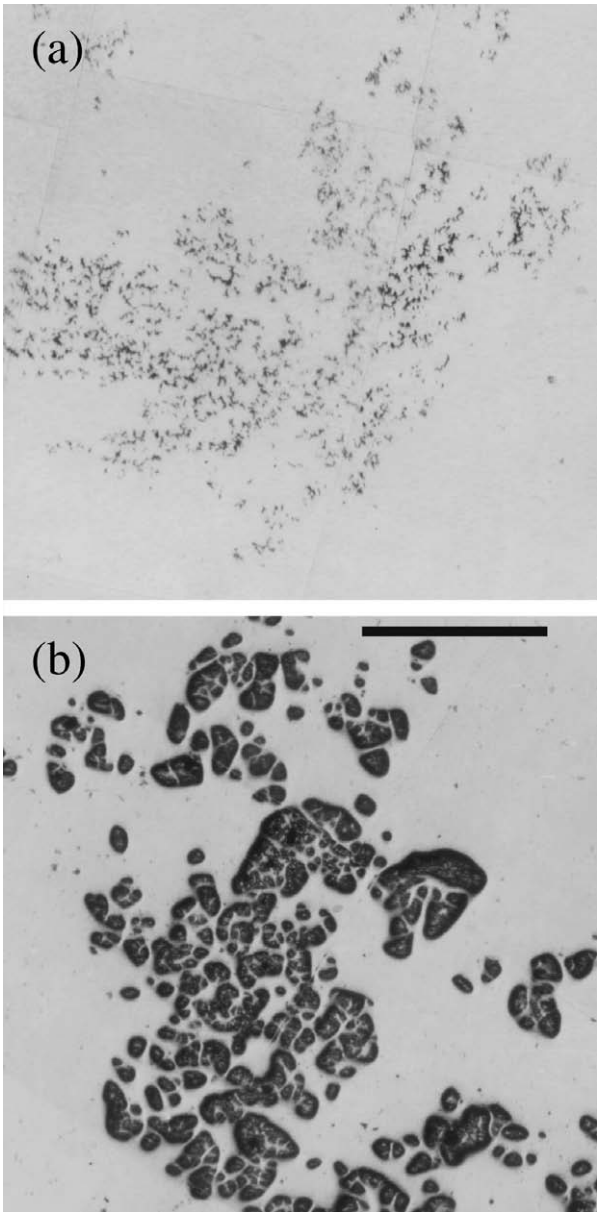

Fig. 1. Microstructure of as-cast fuel pin: (a) top section, (b) lower section. Fiducial Bar = 500 μm.

3.1. Bottom of fuel

The as-cast microstructure at the bottom of the fuel is illustrated by the transverse view in Fig. 2(a). The salient features are a darker gray, irregularly shaped phase in a light matrix. Two areas of mold–melt interaction are arrowed, A and B. At higher magnification (Fig. 3) the irregular phase is found to be composed of a collection of two different smaller particles. Wavelength dispersive spectroscopy (WDS) analysis shown in Fig. 2(b) indicates that the distribution of americium and neptunium is uniform across the section and the light colored smaller (5–15 μm) particles are primarily composed of Zr while the larger dark particles (30–60 μm) have a widely variable composition but contain at most

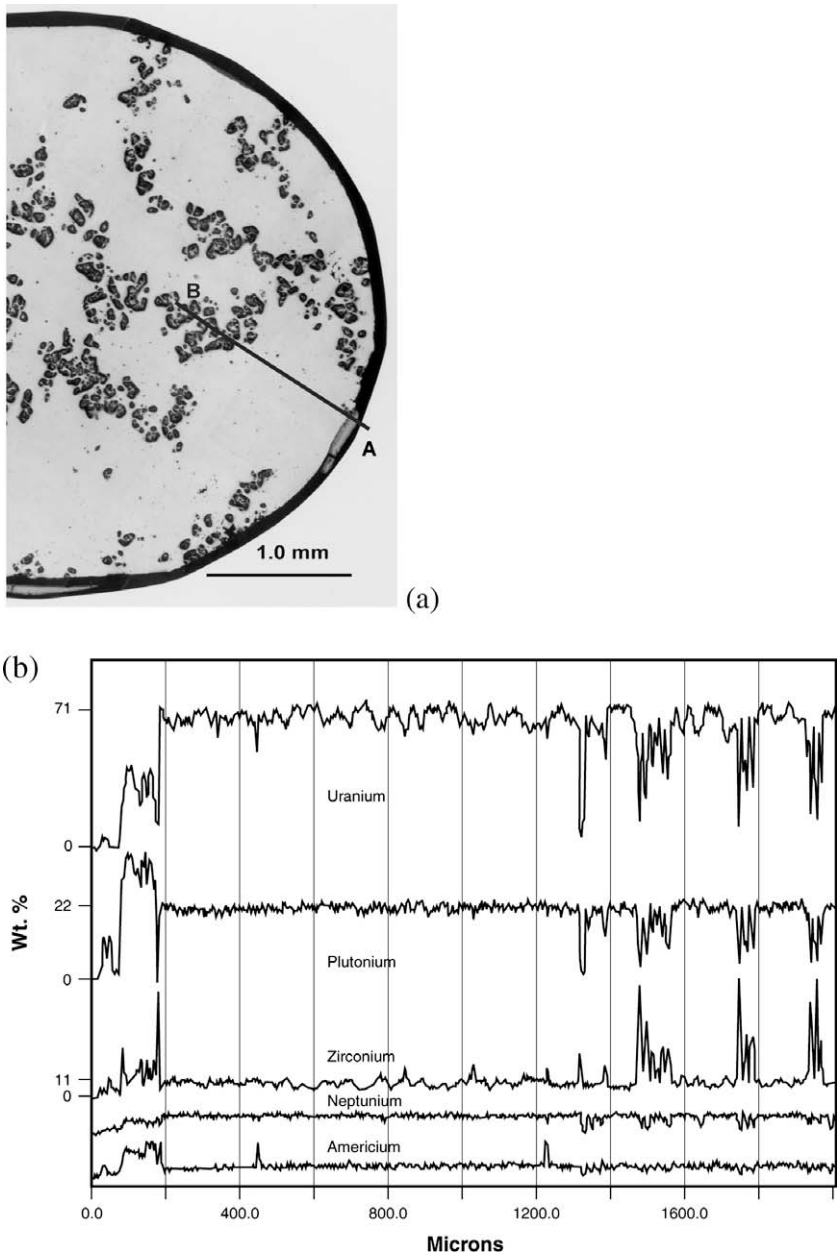

Fig. 2. (a) Transverse optical micrograph of the bottom of the as-fabricated U–20.3%Pu–10.0%Zr–2.1%Am–1.3%Np fuel and (b) wavelength dispersive spectroscopy of A–B line section.

only about 20%Zr. Very fine (0.5–1.5 μm) round particles termed 'beads' were observed internal to the Zr-rich particles and found to be basically composed of U. Examination of the matrix by WDS (wavelength dispersive spectroscopy) revealed that the major constituents did not vary radially across the section. A few high Am peaks were detected, but could not be associated with any particular feature.

3.2. Top of fuel

As seen in Fig. 4(a), the microstructures at the center and top sections of the fuel are analogous. The Zr-rich regions were not collections of irregular particles as seen at the bottom of the fuel, rather the Zr was present mainly in a dendritic morphology. No unusual mold–melt interaction layers were observed and the matrix was uniform in composition as detected by WDS shown in Fig. 4(b).

3.3. Bulk chemistry

Sections from the top, center and bottom of the fuel were chemically analyzed and the results are given in Table 1. The U, Pu, Zr, and Np levels are axially uniform, within experimental error, while the Am level is low in the bottom section of the fuel. Some Am was lost as denoted by the low measured concentrations and is most likely attributed to the casting methods used. Also, there is a notable increase in the amount of Si present in the bottom section versus the top and center sections. Increased Si levels are most likely due to the quartz (SiO,) molds. The ZrO, wash does not completely protect the molds from the mol-

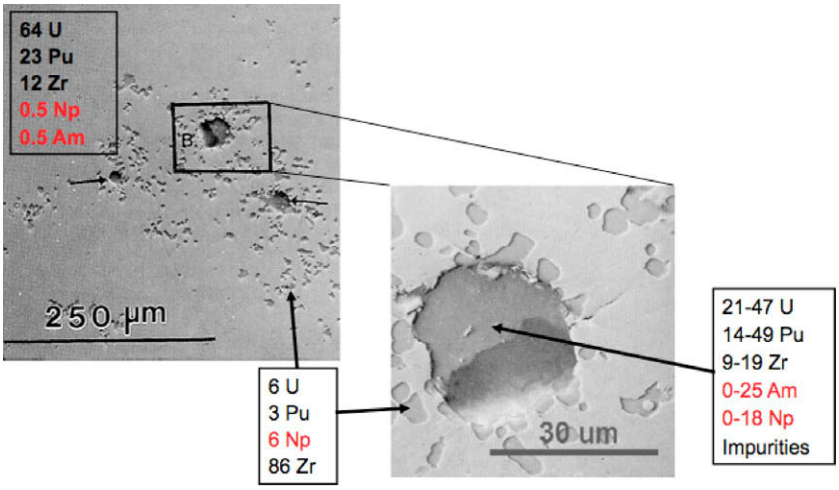

Fig. 3. Individual features in bottom section of the fuel: (a) secondary electron image of the two particle types, (b) higher magnification secondary electron image of area B.

ten fuel and some interaction occurs. Mold–melt interactions are most severe at the bottom of the molds because the mold ends are submerged in the melt for the entire casting time and fuel located at the bottom of the slug cools last after injection casting.

A representative transverse section from a U–20%Pu–10%Zr fuel slug without MA additions is shown in Fig. 5. In this scanning electron microscope image the dark phase is highly rich in Zr (N 80% by weight) akin to the Zr-rich regions observed in the MA-bearing fuel; however, they differ morphologically. In conventional ternary fuel the Zr-rich regions consisted of contiguous globular features, but in the X501 casting these 'globular' regions were broken up into numerous small particles at the bottom of the fuel. This difference in shape could be the result of impurities in the melt.

Conventional U–Pu–Zr fuel contains at most about 300 ppm Si while the fuel in X501 experiment contained up to 14 times more Si. The microchemical analysis revealed impurity segregation in the larger particles (see Fig. 3 and Table 1, i.e., Ca, Si, etc.). This analysis is insensitive to light elements such as C, O, and N and bulk chemical analysis of these elements was not available. Investigations into the U–Zr phase diagram [8] uncovered significant changes in the phase relations at the U-rich end of the phase diagram due to small amounts of oxygen. It is reasonable to expect that the high Si content in the bottom of the fuel would influence the morphology of the Zr-rich phase. Further investigations into the phase relationships in fuel containing impurities, such as Si, O, C, N, and Ca, need to be completed to determine what influence they have on microstructure and phase relationships. The sparking observed during the MA addition was found to be small droplets of the melt emerging from the crucible. Examinations of the inner furnace surfaces and exhaust lines after the casting revealed increased alpha activity from the Am. The 'sparks' were induced by two factors: contaminants in the Pu–Am feed stock with low boiling temperatures and the high vapor pressure of Am at the casting temperature of 1465 °C. The Pu–Am feed stock contained ~3 at.% Ca and Mg (2000 ppm by weight). Both of these elements boil below 1440 °C causing the melt pool to become agitated. Secondly, the equilibrium vapor pressure of Am at 1465 °C is 440 Pa which yields an evaporation rate of about 0.1 g/cm^2 s using the Knudsen–Langmuir equation for pure Am in a vacuum. Considering a crucible with a surface area of 50 cm, an evaporation rate of about 0.1 g/cm^2 s yields a loss of 5 g per second in a perfect vacuum. The present controls on the casting furnace preclude an exact measurement or control of the pressure during casting. A partial vacuum existed prior to placing the molds in the melt. The high vapor pressure of Am at the casting temperature cannot be altered, but large Am losses can be mitigated. Experimentation employing lower superheats would help but may not be feasible because a lower viscosity melt might not completely fill the molds. The total amount of Am lost could also be reduced by further limiting time at temperature and casting under higher positive pressure.

3.4. X501 experiment irradiation

The X501 fuel slugs were fabricated into two EBR-II MkIV con-Fig. fuel pins. The two MA-bearing pins were inserted into a standard EBR-II subassembly with the remainder of the fuel element locations filled with U–10Zr driver fuel. The X501 subassembly was inserted into EBR-II in the central core region, as shown in Fig. 6, beginning in February 1993, and withdrawn just prior to EBR-II shutdown in August 1994. Total irradiation time was 339 EFPD's. Burnup, calculated on the basis of REBUS/RCT/ORIGEN calculations [9] was 7.6% HM with transmutation of 9.1% of ^{241}Am. Peak linear heat generation rate was estimated to be 45 kW/m (13.7 kW/ft) and peak fuel centerline and cladding inner surface temperatures were approximately 700 and 540 °C, respectively. The chemical analysis and physical attributes of the two X501 fuel elements are given in Table 2.

3.5. X501 postirradiation examination

A partial postirradiation examination was completed on X501, including gamma scanning, optical microscopy, microprobe analysis, and metallography. The postirradiation examination completed indicated that the minor additions of Am and Np to the U–Pu–Zr matrix did not effect the irradiation behavior of the fuel.

Gamma scans, example shown in Fig. 7, showed normal metallic fuel fission product behavior, with ^{137}Cs alloying with the bond sodium and migrating to the region near the top of the fuel slug.

A microscopic examination of the inside cladding surface was made to determine if the inclusion of the MA's in U–Pu–Zr fuel has an effect on fuel-cladding-chemical-interaction (FCCI). The HT-9 cladding used for the X501 experiment is also the reference cladding for US transmuter fuel. Optical microscopy (Fig. 8) showed no evidence of reaction layer formation on the inner cladding wall or the outer surface of the fuel slug. A gap is visible between the fuel and the cladding wall at all locations. These preliminary results indicate that under typical metal fuel operating conditions, FCCI with HT-9 is not strongly affected by small amounts of americium or neptunium.

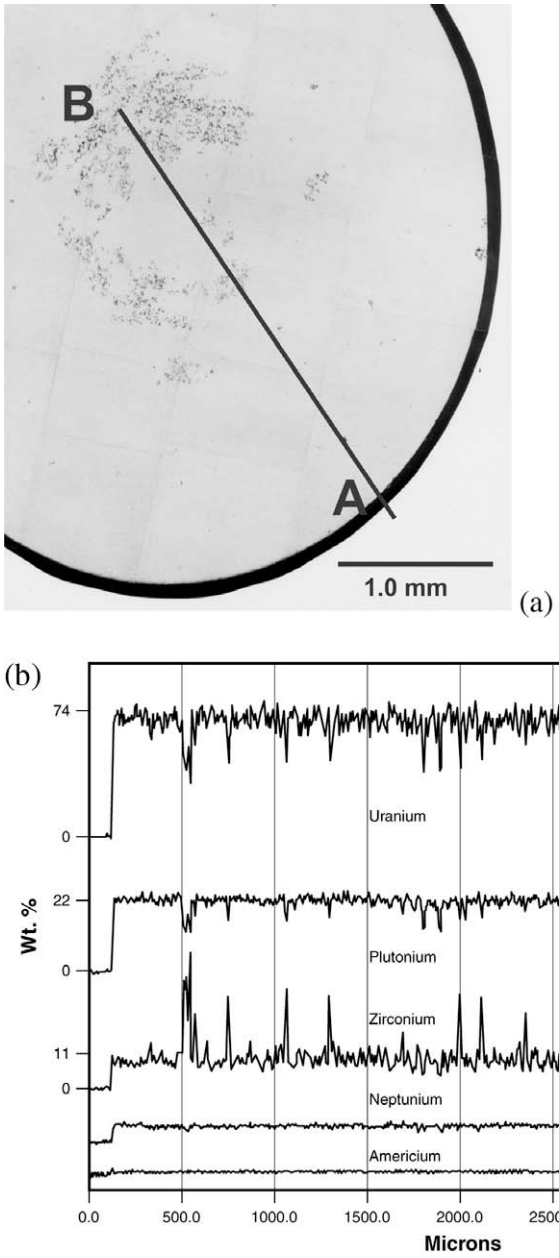

Fig. 4. (a) Transverse optical micrograph of the top of the as-fabricated U–20.3%Pu–10.0%Zr–2.1%Am–1.3%Np fuel casting and (b) wavelength dispersive spectroscopy of A–B line section.

Table 1
Bulk chemical analysis of as-fabricated X501 fuel castings (wt%).

Element	Location			
	Top	Center	Bottom	Average
U	67.31	65.95	68.02	66.06
Pu	19.51	21.24	19.85	20.2
Zr	9.12	9.22	9.02	9.12
Am	1.33	1.32	1.03	1.23
Np	1.39	1.19	1.36	1.31
Si	0.179	0.179	0.422	0.26
Al	0.144	0.077	0.045	0.0887
Ca	0.189	0.0067	0.0046	0.0668
Mg	0.017	0.0028	0.0065	0.0088
Cr	0.0042	0.0018	0.0015	0.0025
Mn	0.0012	0.0009	0.0008	0.001
Fe	0.0018	0.0009	0.0007	0.0011
Ni	0.004	0.004	0.004	0.004

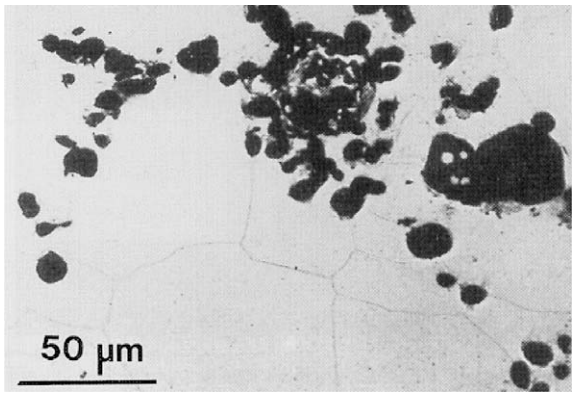

Fig. 5. Micrograph of as-fabricated U–20Pu–10Zr.

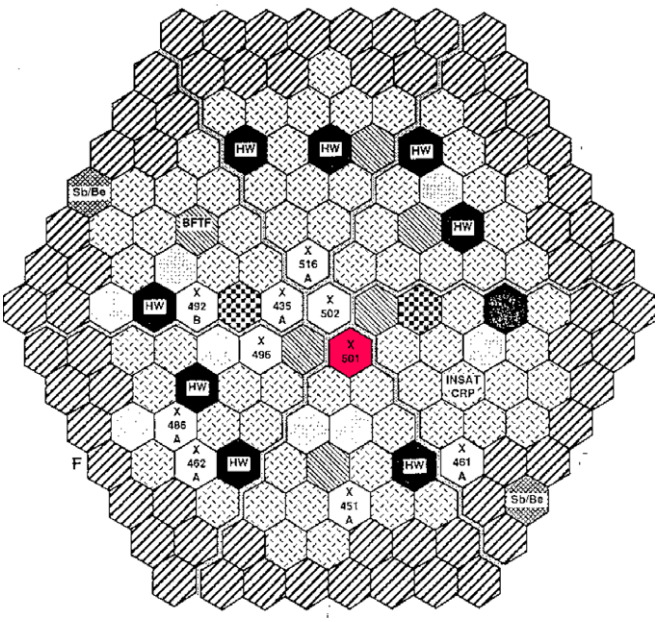

Fig. 6. X501 experiment location in EBR-II.

Table 2
Attributes of X501 minor actinide-bearing fuel elements.

Composition (average analyzed wt%)	U–20.2Pu–9.1Zr–1.2Am–1.3Np
Major impurities (average wt%)	Si:0.26, Al:0.089, Ca:0.067, Cr:0.0025, Mg:0.009, Fe:0.001, Mn:0.001
U-235 enrichment (nominal)	60%
Fuel mass	77.5 g
Fuel length	34.3 cm (13.5 in)
Element length (nominal)	74.9 cm (29.5 in)
Cladding type	HT-9 steel
Cladding OD	5.84 mm (0.230 in)
Cladding wall	0.457 mm (0.018 in)
Slug diameter	4.27 mm (0.168 in)
Plenum volume	7.1 cm^3
Plenum gas	75He–Ar
Smeared density	75%
Fuel slug density, % theoretical	99.5%

Shown in Fig. 9(a) is a postirradiation optical micrograph of a cross section near the center of fuel pin G582. The fuel shows a microstructure typical of U–20Pu–10Zr, where constituent radial redistribution has resulted in the formation of three microstructural zones within the fuel. Fig. 9(b) is a comparison of the WDS traces of neptunium, americium, zirconium, plutonium, and uranium across the section shown in Fig. 9(a). The outer zone, near the cladding, is enriched in zirconium, the intermediate zone is zirconium depleted, and the central zone is enriched in zirconium and depleted in uranium. Plutonium content remains relatively uniform. Americium appears in the WDS traces as features with high elemental concentrations, generally depleted in U, Pu, and Zr (the other major fuel constituents). The morphology of the americium-rich phases cannot be determined from existing micro-

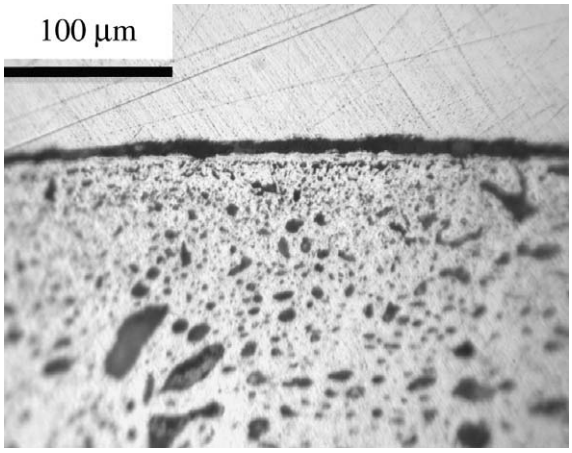

Fig. 8. Optical micrograph of fuel/cladding interface.

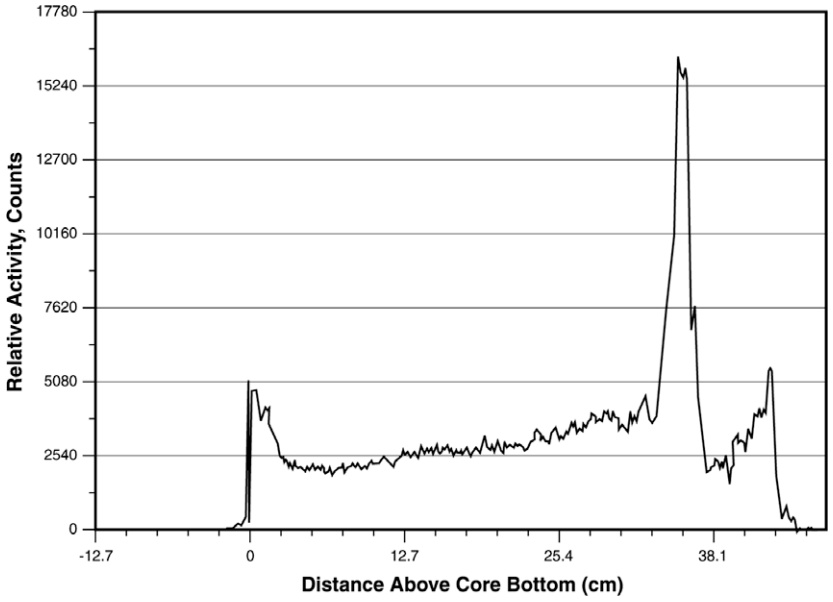

Fig. 7. Example ^{137}Cs gamma scan of a X501 pin.

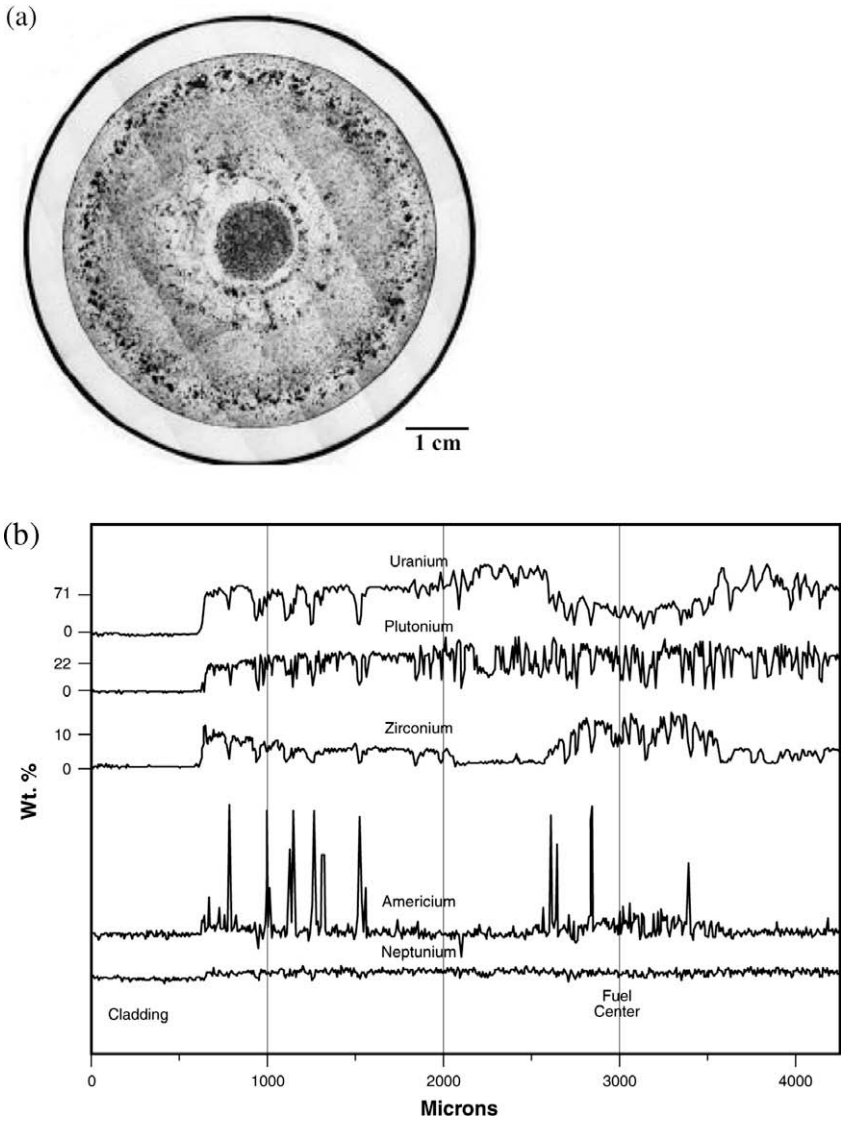

Fig. 9. (a) Postirradiation optical image of MA-bearing fuel and (b) wavelength dispersive spectroscopy line scans showing distribution of actinides and Zr.

graphs, and other elemental constituents, such as fission product and impurity elements were not analyzed during the examination. Comparison of the preirradiation and postirradiation WDS line scans suggests that the americium-rich features formed during irradiation. Americium is present only in the uranium-depleted central and outer zones, indicating that americium migration has occurred along with the migration of uranium and zirconium. Local radial redistribution of americium to the cladding inner wall does not occur; however these results do not rule out the possibility of condensation of americium in the plenum region above the fuel column.

Plenum gas sampling results were combined with ORIGEN calculations to estimate the fission gas and helium release rates from the fuel. Results are shown in Table 3. Helium generation is principally due to a sequence of neutron capture by ^{241}Am, and subsequent decay of the ^{242}Cm product to ^{238}Pu by alpha particle emission. The amount of He introduced as plenum fill gas was estimated based on pressure ratios between fill gas and the quantity of radioactive Xe tag gas measured by counting Xe activity. Based on these estimates, it appears that approximately 90% of the helium gas produced was released to the plenum. Fission gas release was 79%, typical of U–Pu–Zr fuel at this burnup.

The generation of helium gas during transmutation of ^{241}Am is a significant issue that must be considered in the design of transmuter fuel. In fuels with high americium content, helium generation is principally due to neutron capture by ^{241}Am and subsequent alpha decay of ^{242}Cm to ^{238}Pu. There are three known experiments involving transmutation of ^{241}Am. Helium release results from two, the EFTTRA-T4 test and the SUPERFACT-1 experiment have been previously published. Some data on helium generation is available for each experiment, and results are presented in Table 4, along with ORIGEN calculations for the US Na-cooled point design and X501 data. The quality and completeness

Table 3
X501 gas production and release.

BOL ^{241}Am content	0.972 g
EOL ^{241}Am content	0.884 g
^{241}Am transmutation	0.088 g (9.1%)
Measured He release	3.1 cm^3
Calculated He inventory, 1 year decay	3.4 cm^3
He release	90%
FG release	79%

Table 4
Data and calculations for He production in ^{241}Am-bearing fuels.

Experiment	Specific He generation (ml per g ^{241}Am transmuted)
X501	38.6–44.8
SUPERFACT-1	33.3–63.4
EFTTRA-T4	44.8–59.9
Na point design	58.1

of data vary for each experiment; therefore the results of this analysis contain a good deal of uncertainty, and do not provide a good basis for extrapolation. A rule-of-thumb for estimating helium production from americium for the US transmuter design, based on the results in Table 4 and calculations of compositions ranging from 6 to 40 wt% ^{241}Am is 50 cm^3 He per gram of transmuted americium. The wide range of possible fuel compositions leads to a wide range in the potential for helium production. Helium production is likely to be the most important fuel design consideration for transmutation scenarios with high MA content.

4. Conclusion

The US fast reactor fuel program demonstrated the use of americium-bearing fuel in the early 1990s. Three full length fuel pins containing minor actinide additions were successfully cast with no unusual macrosegregation of major constituents observed. The Zr-rich phase displayed an unconventional morphology in the bottom section of the castings, appearing as a dense collection of small particles instead of the usual contiguous globular shape. This is probably the result of significant levels of impurities present. Approximately 40% of the initial Am charge was lost during casting due to volatile impurities (Ca and Mg) in the Am–Pu feed stock and through evaporation. Limited postirradiation examination results from the X501 experiment indicate that the addition of 1.2 wt% of americium did not alter the behavior of metallic U–Pu–Zr fuel.

US Department of energy disclaimer

Acknowledgments

This submitted manuscript has been authored by a contractor of the US Government for the US Department of Energy, Office of Nuclear Energy, Science, and Technology (NE), under DOE–NE Idaho Operations Office Contract DE-AC07-05ID14517. Accordingly, the US Government retains a nonexclusive, royalty-free license to publish or reproduce the published form of this contribution, or allow others to do so, for US Government purposes.

The authors wish to acknowledge C.L. Trybus for preparing the X501 experiment for irradiation. The work presented in this report represents the efforts of many researchers, technicians, as well as the efforts of EBR-II operations personnel. Their efforts should be recognized.

References

[1] Y.I. Chang, Nucl. Technol. 88 (1989) 129.
[2] A.G. Croff, C.W. Forsberg, S.B. Ludwig, in: Proceedings of the ANS Meeting, November 1990, Washington DC, CONP-901101, 1990, p. 144.
[3] Y.I. Chang, C.E. Till, in: Proceedings of the Annual WATTec Conference and Exhibition, February 1989, Knoxville, TN, CONF-890218-13, 1989, p. 129.
[4] C.L. Trybus, J.E. Sanecki, S.P. Henslee, J. Nucl. Mater. 204 (1993) 50.
[5] N.D. Erway, O.C. Simpson, J. Chem. Phys. 18 (1950) 953.
[6] C.B. Alock, V.P. Itkin, M.K. Horrigan, Can. Metall. Quart. 23 (3) (1984) 309.
[7] E.H.P. Cordfunke, R.J.M. Konings (Eds.), Thermochemical Data for Reactor Materials and Fission Products, North-Holland, Amsterdam, 1990.
[8] S.T. Zegler, USAEC Report ANL-6055, 1962.
[9] R. McKnight, Argonne National Laboratory, personal communication, 2001.